

Subaru Observations for the K -Band Luminosity Distribution of Galaxies in Clusters near to 3C 324 at $z \sim 1.2$

Masaru KAJISAWA, Toru YAMADA, Ichi TANAKA
Astronomical Institute, Tohoku University, Aoba-ku, Sendai 980-8578
E-mail(MK): kajisawa@astr.tohoku.ac.jp

Toshinori MAIHARA, Fumihide IWAMURO, Hiroshi TERADA, Miwa GOTO,
Kentaro MOTOHARA, Hirohisa TANABE, Tomoyuki TAGUCHI, Ryuji HATA
Department of Physics, Faculty of Science, Kyoto University, Sakyo-ku,
Kyoto 606-8502

Masanori IYE, Masatoshi IMANISHI, Yoshihiro CHIKADA
National Astronomical Observatory, 2-21-1, Osawa, Mitaka, Tokyo 181-8588

Chris SIMPSON, Toshiyuki SASAKI, George KOSUGI, Tomonori USUDA,
Tomio KANZAWA and Tomio KURAKAMI
Subaru Telescope, National Astronomical Observatory of Japan,
650 North Aohoku Place, Hilo, HI 96720, U.S.A.

(Received 1999 September 3; accepted 1999 December 22)

Abstract

We investigate the K -band luminosity distribution of galaxies in the region of clusters at $z \sim 1.2$ near to the radio galaxy 3C 324. The imaging data were obtained during the commissioning period of the Subaru telescope. There is a significant excess of the surface number density of the galaxies with $K = 17\text{--}20$ mag in the region within $\sim 40''$ from 3C 324. At this bright end, the measured luminosity distribution shows a drop, which can be represented by the exponential cut off of the Schechter-function formula; the best-fitted value of the characteristic magnitude, K^* , is $\sim 18.4 \pm 0.8$. This measurement follows the evolutionary trend of the K^* of the rich clusters observed at an intermediate redshift, which is consistent with passive evolution models with a formation redshift $z_f \gtrsim 2$. At $K \gtrsim 20$ mag, however, the excess of the galaxy surface density in the region of the clusters decreases abruptly, which may imply that the luminosity function of the cluster galaxies has a negative slope at the faint end. This may imply strong luminosity segregation between the inner and outer parts of the clusters, or some deficit of faint galaxies in the cluster central region of the cluster.

Key words: galaxies: evolution — galaxies: formation — galaxies: luminosity function, mass function

1. Introduction

The luminosity function (LF) is one of the basic probes for studying galaxy formation. Particularly, the near-infrared K -band LF can be used as a tracer of the galaxy mass distribution since the near-infrared light of a quiescent galaxy is dominated by low-mass stars, and can be an approximate measure of the total stellar mass. Hierarchical structure formation models can be directly tested by observing the evolution of near-infrared LF over a significant redshift range (e.g., Kauffmann et al. 1993).

Near-infrared observations also have some practical ad-

vantages when one investigates the LF of galaxies at high redshift; it provides a relatively uniform and unbiased measure of the galaxy luminosity distribution, since the galaxy luminosity in the K -band is much less sensitive to the on-going star-formation activity, the scale of which may vary from galaxy to galaxy; also, the K -correction factor is relatively small and nearly independent of the Hubble type, even at large redshifts.

Observing the near-infrared LF in high-redshift-rich clusters may constrain the history of the evolution of the galaxy mass distribution in the highest density environment in the Universe. De Propris et al. (1999)

recently investigated the evolution of the K -band LF of galaxies in rich clusters at $z=0.1$ – 0.9 . The measured LF can be fitted by the Schechter function, and the behavior of the characteristic magnitude, K^* , along redshift is consistent with those predicted by the passive-evolution models with a single starburst at $z=2-3$. Combining these results with the mild evolution of the mass-to-light ratio of the cluster elliptical galaxies, they concluded that the assembly of galaxies at the bright end of the LF was largely completed by $z \approx 1$.

Pushing these studies toward higher redshift constrains the formation history of galaxies in clusters more strongly. In a general field environment, Kauffmann and Charlot (1998) claimed a deficit of red giant elliptical galaxies at $z \gtrsim 1$. Franceschini et al. (1998) also argued that the number density of bright elliptical galaxies significantly decreases above $z \sim 1.3$. Although there is still much debate on these subjects (e.g., Totani, Yoshii 1998), it would be interesting to also study the K -band LF of galaxies in rich clusters at $z \gtrsim 1$. Observing rich clusters has an advantage, because the galaxies are at a single distance and the LF can be evaluated by measuring the galaxy surface-density excess of the cluster region over the non-cluster region, while it is still a time-consuming task to spectroscopically measure the distances to each individual galaxy in the field. The disadvantage is that the uncertainty of the field correction could seriously affect the results, especially at the faintest end where the galaxy counts may be dominated by the foreground/background galaxies.

Recently, more than several clusters and cluster candidates at $z \gtrsim 1$ have been discovered (Dickinson 1995; Yamada et al. 1997; Stanford et al. 1997; Hall, Green 1998; Benítez et al. 1999; Rosati et al. 1999). Most of these objects have been selected or identified by the surface density excess of the quiescent old galaxy population. Near-infrared luminosity distributions of the galaxies in these high-redshift clusters, however, have so far not been studied intensively.

In this paper, we present the K -band luminosity distribution of the galaxies in the clusters at $z \sim 1.2$ near to the radio galaxy 3C 324 using the images obtained with the Subaru telescope. These clusters are recognized by Kristian et al. (1974) and by Spinrad and Djorgovski (1984), and firmly identified by Dickinson (1995). The clusters have been spectroscopically confirmed, and the surface-density excess was revealed to be due to the superposition of two systems at $z = 1.15$ and $z = 1.21$ (Dickinson 1997a, b). The extended X-ray emission, whose luminosity is comparable to that of the Coma cluster, has been detected toward the direction of 3C 324 (Dickinson 1997a), which indicates that at least one of the two systems, probably the $z = 1.21$ one in which 3C 324 exists, is a fairly collapsed massive system. Smail and Dickinson (1995) detected a weak shear pattern in the field

that may be produced by a cluster associated with 3C 324. We describe the observation and the data reduction briefly in section 2. In section 3, we present the obtained K -band luminosity function and the surface number density distribution. Our conclusions and the discussions are given in the last section.

2. Observations and Data Reduction

The 3C 324 field was observed at the K' band with the Subaru telescope equipped with the Cooled Infrared Spectrograph and Camera for OHS (CISCO, Motohara et al. 1998) on 1999 March 31 and April 1, during the telescope commissioning period. The detector used was a 1024×1024 HgCdTe array with a pixel scale of $0''.116$, which provides a field of view of $\sim 2' \times 2'$. A number of dis-registered images with short exposures (20 s for each frame) were taken in a circular dither pattern with a $10''$ radius; a series of twelve frames were taken at one place and the telescope was then moved to the next position. The total net exposure time was 3000 s. The weather condition was stable during the observations, and the seeing was $\sim 0''.8$ on March 31 (1600 s) and between $0''.3$ and $0''.5$ on April 1 (1400 s).

The data were reduced using the IRAF software package. There was a variation in the bias level of CISCO during the observations and the residual pattern is not flat and makes a 10–20% discontinuity of the background level in each frame at the boundary of the quadrants of the array at the central column of the detector. In the first and the second frames of the series of the twelve exposures taken at one position, the residual is much smaller than those in the following other frames. We thus made the ‘template’ bias frame, which was to be scaled and subtracted from all frames, by subtracting the first frame of the series averaged over the observations from the average of the third to twelfth frames. Flat fielding was performed using the frame constructed from our own data by median stacking of the bias-subtracted images after masking out the tentatively detected objects. As a check, we compared our flat-fielding frame with that constructed from many other frames taken with CISCO by the time of the observations (made by the CISCO team), and found that their difference was less than 5%. We indeed performed the same analysis using this general flat-fielding frame, and found no systematic difference in the results. After the flat-fielding, by fitting the background with the 10th-order surface function after masking the detected objects, we subtracted the sky background and the remaining slight distortion near to the central column due to the bias variation and a small pattern of an unfocused image, which was probably caused by a piece of dust on the camera window, and appeared in the top-left quadrant of the frame during our observations. Since the fitted surface was smooth and had a small gradient over

the frame, except for the regions of the dust pattern and near to the central column, source detection and photometry were little affected by this procedure. As a further check, we also performed the median-sky (prepared from the disregistered data frames) subtraction before removing the spurious patterns by the surface fitting, and found little difference in the results. The resultant frames were convolved with the Gaussian kernel in order to match the FWHM of the stellar images to the worst one ($0.''8$). They were then co-registered and normalized to be median stacked.

The flux densities of the detected sources were calibrated to those in the *K*-band by using a star in the list of UKIRT Faint Standards, FS 27 ($K - K' = -0.01$), observed just after the 3C 324 field at a similar zenith distance. Since the true-color term of the telescope and the instrument has not been defined at this stage, and we do not have infrared colors of the objects, no color correction was applied. Using the model spectra and the transmission curve of the CISCO K' filter, we evaluated $K - K' \sim -0.1$ for an old passively evolving galaxy at $z = 1.2$. Many foreground galaxies may have bluer infrared spectra and the color correction may be smaller than this. We checked the stability of the results presented below by artificially shifting the magnitude zero point by 0.1–0.2 mag, and confirmed that they are little affected by the procedure.

We used the SExtractor software (Bertin, Arnouts 1996) to detect the objects in our image. A detection threshold of $\mu_K = 22.4$ mag arcsec $^{-2}$ over 20 connected pixels was used. Photometry was made with $3''$ diameter apertures. We removed the bright objects with $K < 18$, whose light profile is consistent with the stellar ones from the final galaxy catalog. We did not make any star/galaxy separation at the fainter magnitude, but the contribution of the stars was small at $K > 18$ and at most $\sim 5 - 10\%$ (De Propriis et al. 1999). A total of 146 sources were cataloged.

Figure 1 shows the distribution of the detected objects on the sky. The position angle of the frame is 218° . We show the objects with $K < 20$ mag by the filled circles and those with $K > 20$ by the open ones. In order to evaluate the completeness of the object detection, we performed a simulation using the IRAF ARTDATA package. An artificial galaxy with a given apparent magnitude is generated and added on the observed frame at random coordinates, and the source-detection procedure with the same threshold was performed to check whether the artificial object can be detected or not. By repeating this procedure, we estimated the probability that a galaxy with a given magnitude is detected. Each artificial galaxy has a light profile with parameters randomly selected from the range of half-light radius between $0.''1$ and $0.''8$ (corresponds to 0.9–6.9 kpc at $z = 1.2$ for $H_0 = 50$ km s $^{-1}$ Mpc $^{-1}$ and $q_0 = 0.5$) and that of the axial ratio

between 0.3 and 1.0. While the range of the radius was chosen to represent typical galaxies at $z = 1.2$, it covered the size of the typical field galaxies. Yan et al. (1998) showed that the size of galaxies with $H = 19$ – 23 mag (roughly corresponding to $K = 18$ – 22 mag) is between $0.''2$ and $0.''6$. The seeing effect was taken into account by convolving the model-galaxy image with the Gaussian kernel. The result is shown in figure 2. They are equally-weighted averaged values for the model galaxies with various sizes and axial ratios. The detection completeness was $\sim 90\%$ at $K = 21$ mag and still $\sim 70\%$ at $K = 21.5$ mag; we use the average value for the disk and de Vaucouleurs profiles in the rest of this paper.

The detection completeness is low for the low surface brightness galaxies. It may become $\sim 70\%$ and $\sim 50\%$ at $K = 21$ and 21.5 mag, respectively, if we assume an effective radius between $0.''7$ and $0.''8$. This, however, certainly underestimates the true completeness value, since the faint galaxies have generally smaller sizes of $\sim 0.''3$ – $0.''4$ at $H = 22$ mag (Yan et al. 1998).

3. Results

Figure 3 shows the differential number counts of galaxies detected on the entire field of the CISCO K' -band image. The counts were made by 0.5 mag step with one magnitude bin. For a comparison, those obtained in the general fields taken from various literatures are also shown. The corrected counts of the frame are fairly consistent with those of the Hawaii Deep Survey (Cowie et al. 1994) and in Moustakas et al. (1997) at $K \gtrsim 22$ mag, where the galaxy counts may be dominated by the foreground/background galaxies. Bershadsky et al. (1998) gives systematically higher counts than others, which may be due to the large-scale structures in the galaxy distribution and the small area of the observed regions.

In figure 4, we show the galaxy surface-density profile in the frame as a function of the distance from 3C 324 for those objects with $K = 17$ – 20 mag. The dashed line shows the averaged field surface density obtained from the literature shown in figure 3. There is a conspicuous surface-density excess of galaxies within $\sim 40''$ from 3C 324. The radius corresponds to ~ 0.35 Mpc at $z \sim 1.2$. This result is consistent with those presented in figure 3 of Dickinson (1997b). Dickinson (1997b) also revealed that the galaxies within $30''$ radius from 3C 324 show strong peaks at $z = 1.21$ and 1.15 in the redshift distribution. In the following discussion we do not distinguish the two systems at $z \sim 1.2$, since the detailed redshift distribution of the galaxies or the relative population of them is still unknown. Namely, we discuss the average properties of the two clusters. Since their redshifts are close, it little affects the discussion about the absolute luminosity and the color distributions. In fact, it is a common technique to combine a few clusters at similar redshifts to reduce

the statistical fluctuation of the galaxy counts.

We tentatively divide the observed field into the “cluster” region, which is the region within 40” radius from 3C 324 (shown by the large circle in Figure 1), and the adjacent “outer” region, which is the remaining region of the frame. The area of the cluster and the outer regions are 1.433 arcmin² and 1.981 arcmin², respectively, and 71 galaxies are in the cluster region. In figure 5, we show the differential number counts for the two regions separately as well as the average counts in the literature shown in figure 3, approximated by the straight line fitted at $K > 17$ mag. In fitting the average field counts, we put weights by the errors of the values in order to minimize the effect of the uncertainties in the incompleteness correction for the data in the literature. Here we plotted the density normalized for the area of the cluster region so that the readers can see the true numbers of galaxies detected on our frame in each magnitude bin. As expected from figure 4, the excess of the galaxy surface density of the cluster region is clearly seen at $K \sim 17$ –20 mag. On the other hand, the counts of the outer region are similar to the general field counts over the entire magnitude range, and are likely to be dominated by the foreground/background field galaxies.

At $K \sim 20$ –21 mag, the excess of the surface number density of the cluster region decreases very rapidly, and the density even becomes consistent with those of the field at $K = 21$ mag. The slope of the counts between $K = 19$ mag and 21 mag in the cluster region becomes fairly flat while the counts of the outer region keeps rising with a similar slope as in the general fields.

The decline of the counts could be due to detection incompleteness at the crowded region. To check this, we show the evaluated detection completeness as a function of the radius from 3C 324 (figure 6). It can be seen that the detection completeness for the galaxies with $K = 20$ –22 mag only marginally decreases toward 3C 324, except for the innermost bin within 10” radius where the effect of the host of 3C 324, which is the brightest cluster galaxy in the system at $z = 1.21$, becomes large and an $\sim 20\%$ decrease of the completeness is seen.

Figure 7 shows the obtained luminosity distribution of the galaxies in the “cluster” region. For the field correction, the average counts shown in figure 5 are used. It shows some cut-off at the bright end, and also drops abruptly toward the fainter magnitude at $K \sim 20$ mag. We fitted the Schechter function, $\Phi(L) = \phi^* (\frac{L}{L^*})^\alpha \exp(-\frac{L}{L^*})$, (Schechter 1976), to the bright end of the luminosity distribution using the data points in the range of 17–20 mag in order to compare the results with those obtained in a similar manner for the lower redshift clusters in De Propris et al. (1999) (but there is a discrepancy in that we treat the differential number counts here, while De Propris et al. (1999) investigated the cumulative ones). The faint-end slope of the

Schechter function, $\alpha = -0.9$, is assumed as in De Propris et al. (1999). Although the fitting is far from perfect, the drop toward the brightest end can be represented by the exponential cut off, as in the Schechter function. The characteristic magnitude derived in this procedure is $K^* = 18.4 \pm 0.8$ mag.

The apparent rapid drop in the luminosity distribution at $K = 20$ –21 mag seems to be conspicuous. If we assume $\alpha = -0.9$, the expected number of the cluster galaxies per magnitude is ~ 9.1 at $K = 21$ mag, while the observed count between $K = 20.5$ and 21.5 mag is negative after a field correction. The detection completeness is still ~ 95 –70% at this depth, and may not be much affected by the uncertainties in the incompleteness correction. The expected average number of field galaxies is 22.8 per magnitude at $K = 21$ mag, while the observed count is 18 and to be 21.6 after the incompleteness correction. If this behavior is due to a fluctuation of the foreground/background galaxy counts, there must be a sudden deficit of about ten galaxies per magnitude just below ~ 20 mag and just inside the 40” radius from 3C 324. If we assume that there are 9.1 cluster galaxies in the region, the corresponding number of ‘observed’ field galaxies is 12.5. If the number density of the field galaxies follows Poisson statistics, the confidence level of the lower limit (12.5 galaxies) is 99.5% for $n = 23$. If we assume the presence of 12 and 6 cluster galaxies (9 ± 3 galaxies), the corresponding number of field galaxies is 9.6 and 15.6, respectively, and the confidence level is 99.98% and 95.0%. If we assume that the sum of the cluster and field galaxy counts approximately follow Poisson statistics, the expected number of galaxies per magnitude at $K = 21$ mag is 31.9 for $\alpha = -0.9$. The confidence level for the lower limit (21.6) is then 97.7%. Thus, in fact, the formal significance of the deficit of cluster galaxies is not very large. In the real universe, the distribution of galaxies is more inhomogeneous and the significance may be even lower. However, there is also no reason that such a relatively rare deficit occurs just in the ‘cluster’ region where the brighter galaxies are strongly clustered. We therefore argue that the absence of any number count excess at $K = 21$ relative to the expected field galaxy counts is instead an intrinsic property of the cluster. We can investigate this further by using the color information for the galaxies. Indeed, we found four galaxies in the ‘cluster’ region whose $B - R$ and $R - K$ colors are consistent with those of the galaxies at $z = 1.2$ or higher redshift (Kajisawa et al. 2000), although we do not see how many of them indeed belong to the clusters and how many are background galaxies. The true number of cluster galaxies can only be determined by future complete spectroscopic surveys or more accurate photometric redshift measurements.

How stable are these results in spite of the non-negligible uncertainty of the applied field correction ?

The galaxy counts of the “outer” region of the frame may provide another representative field correction. Although there is a disadvantage that the statistical uncertainty is large especially at the bright end, due to the small number of the objects, there is an advantage that the foreground/background galaxies in the outer region share similar large-scale structures with those in the adjacent cluster region. Furthermore, they also share any possible systematic errors in our data reduction and analysis. At the bright end, $17 < K < 20$, the counts in the outer region are 10–50 % smaller than the average field counts. This does not change the resultant luminosity distribution of the cluster galaxies very much, since the number of cluster galaxies is much larger than both the number densities of the outer region and the average field. On the other hand, at $20 < K < 21.5$, where the deficit of the cluster galaxies is observed, the number density of the outer region is very similar to that of the average field (figure 5). Thus, the resultant luminosity distribution does not change very much at $K \lesssim 21.5$ if we use the counts in the outer region on the same frame instead of the average field counts for the field correction.

We also examined the surface density profile of faint galaxies with $K = 20$ – 22 mag (figure 8). The raw counts as well as those corrected using the results shown in figure 6 are plotted. The surface density within $40''$ radius from 3C 324 is even consistent with those of the field, either the average one or the counts in the “outer” region in the same frame. We show the expected surface-density profile within $40''$ radius scaled from the excess counts at $K = 17$ – 20 mag assuming the slope of the faint end of LF, ($\alpha=0, -0.9, -1.4$), and the characteristic magnitude, $K^* = 18.4$ mag. The case of $\alpha = -1.4$ cannot be compatible with the observed data. Even for the case of $\alpha = -0.9$, the observed points are systematically smaller than the expected counts, although the trend is somewhat marginal. The observed data seems to be more consistent with the case of $\alpha = 0$, or even that of no surface density excess.

It is difficult to constrain the further faint end of the LF below $K \sim 22$ mag, since the galaxy counts are dominated by the foreground/background galaxies, even in the “cluster” region, and the uncertainty of the incompleteness correction may also greatly affect the results. We note, however, that the surface density of the detected objects in the cluster region is systematically higher than that of the outer region at $K = 21.5$ – 23 mag. Some excess of the cluster galaxies could exist at this magnitude range.

4. Conclusion and Discussions

We presented the luminosity distribution and the surface-density distribution for the *K*-band selected galaxies in the region of the clusters at $z = 1.15$ and 1.21

near to the radio galaxy 3C 324. While the bright end of the luminosity distribution can be represented by the Schechter-function-like exponential cut off with a characteristic magnitude of $K^* \sim 18.4$ mag, a rapid decrease in the surface-density excess compared to the average field counts is also seen at the faint end below $K \sim 20$ mag, ~ 1.5 magnitude fainter than K^* .

Figure 9 compares the obtained value of K^* with those of the lower-redshift clusters studied by De Propriis et al. (1999). Various lines in the figure show the behavior expected for the no-evolution and the passive-evolution models with various cosmological parameters calculated by using GISSEL96 (Bruzual, Charlot 1993). Following De Propriis et al., we used a 0.1 Gyr burst model with a Salpeter IMF and with solar metallicity. It can be seen that our result follows the trend of the intermediate-redshift clusters that is consistent with the passive evolution models with star-formation epoch of $z \gtrsim 2$. At $K \lesssim 20$ mag, the dominant population in the clusters of 3C 324 seems to be old quiescent galaxies which were formed at least ~ 1 Gyr ago from the observed epoch.

The faint-end slope of the optical and near-infrared LF of the nearby and intermediate-redshift clusters has been studied extensively (Sandage et al. 1985; Thompson, Gregory 1993; Driver et al. 1994; Kashikawa et al. 1995; Biviano et al. 1995; Secker, Harris 1996; Metcalfe et al. 1994; Barger et al. 1996; Smith et al. 1997; Wilson et al. 1997; Driver et al. 1998). Through near-infrared observations, Barger et al. (1996) give $\alpha = -1$ for the *K*-band LF of the $z \sim 0.31$ clusters. There is no such deficit as seen in the 3C 324 clusters at the magnitude range between M_K^* and $M_K^* + 3$. Wilson et al. (1997) also give $\alpha = -1$ and -1.3 for the *I*-band LF of the two clusters at $z \sim 0.2$, respectively. Although there are some unevenness within a factor of two, no rapid drop is seen between m_I^* and $m_I^* + 4$.

There is evidence that the optical LF of the clusters may be bimodal and better fitted by the combination of a Gaussian distribution for the bright (giant) galaxies and the Schechter function for the faint (dwarf) galaxies rather than by the single Schechter function (Sandage et al. 1985; Thompson, Gregory 1993; Kashikawa et al. 1995; Biviano et al. 1995; Secker, Harris 1996; Metcalfe et al. 1994). Indeed, both the *B*-band and *R*-band LFs of the Coma cluster show some ‘gap’ at ~ 1 mag fainter than the peak magnitude of the bright population (Biviano et al. 1995; Secker, Harris 1996). In the *R* band, the characteristic magnitude of the ‘faint’ population is ~ 1 – 1.5 mag fainter than the peak magnitude of the ‘bright’ one (Secker, Harris 1996). The shape of the *H*-band luminosity function of the Coma cluster (De Propriis et al. 1998) is also consistent with these results.

On the other hand, a deficit of the galaxies is seen at ~ 1.5 – 2.5 mag fainter than the K^* in the 3C 324 clusters. Although there is still an uncertainty of ~ 1 mag in the

value of the K^* , the deficit of the galaxy seems to occur at the magnitude range where the dwarf population already begins to dominate in the Coma cluster. How can we interpret this deficit of the faint galaxies at $K \sim 21$ in the 3C 324 clusters if it is not just a statistical fluctuation of the foreground/background galaxies and an intrinsic property of the cluster?

It may be due to luminosity segregation between the inner and outer radius from 3C 324. The physical diameter of the “cluster region” ($R < 40''$) studied in this paper is ~ 0.7 Mpc, and thus should be considered to be a central part of the cluster. Driver et al. (1998) have shown that the dwarf galaxies ($M_R > M_R^* + 3$) are less concentrated than the luminous galaxies in the clusters with Bautz–Morgan type III, namely, irregular less-concentrated systems. The rich clusters at high redshift may still be dynamically young and share the properties of irregular clusters seen in the local universe. If the faint galaxies in the 3C 324 clusters are more populous in the outskirts region, or distributed rather flat over the scale of a few Mpc, the excess of the surface density can be easily hidden by the numerous foreground/background galaxies.

Another possibility is the intrinsic deficiency of the faint galaxy population in the cluster(s). There is a model involving a late formation of dwarf galaxies. Kepner et al. (1997) have shown that the UV background radiation of $J_\nu = 10^{-21}$ erg s $^{-1}$ cm $^{-2}$ Hz $^{-1}$ at the Lyman limit at $z = 3$ and evolves as $(1 + z)^4$ can prevent a baryonic collapse in the dark-matter halo with a circular velocity of $\lesssim 30$ km s $^{-1}$ by $z \sim 1.5$, although the Hubble Deep Field observation did not prove the presence of many ‘bursting dwarf’ populations (Ferguson, Babul 1998). The circular velocity, ~ 30 km s $^{-1}$, corresponds to the dynamical mass of $\sim 10^9 M_\odot$, or may be $L \sim 0.01 L^*$ and much less luminous than the $K \sim 21$ mag object ($\sim 0.1 L^*$). In a rich cluster environment at a high redshift, however, the limiting mass could be larger, since there may be large extra contribution of UV radiation by the massive stars rapidly formed in the primordial giant elliptical galaxies, which constitute the bright end of the LF at the observed epoch, in addition to the general background field, which may be due to quasars.

The results presented in the paper are just for one region and the superposition of the two distinct systems could make the situation more complex. Clearly, it is important to extend the study of the LF to other high-redshift clusters as well as to constrain more firmly the faint-end of the LF in the intermediate-redshift clusters.

We would like to thank the referee, Mark Dickinson for his invaluable comments. The present result is indebted to all the members of the Subaru Observatory, NAOJ,

Japan. This research was supported by grants-in-aid for scientific research of the Japanese Ministry of Education, Science, Sports and Culture (08740181, 09740168). This work was also supported by the Foundation for the Promotion of Astronomy of Japan. The Image Reduction and Analysis Facility (IRAF) used in this paper is distributed by National Optical Astronomy Observatories, operated by the Association of Universities for Research in Astronomy, Inc., under contact to the National Science Foundation.

References

- Barger A. J., Aragón-Salamanca A., Ellis R. S., Couch W. J., Smail I., Sharples R. M. 1996, MNRAS 279, 1
- Benítez N., Broadhurst T., Rosati P., Courbin F., Squires G., Lidman C., Magain P. 1999, ApJ 527, 31
- Bershady M. A., Lowenthal J. D., Koo D. C. 1998, ApJ 505 50
- Bertin E., Arnouts S. 1996, A&AS 117, 393
- Biviano A., Durret F., Gerbal D., Le Fevre O., Lobo C., Mazure A., Slezak E. 1995, A&AS 297, 610
- Bruzual A. G., Charlot S. 1993, ApJ 405, 538
- Cowie L. L., Gardner J. P., Hu E. M., Songaila A., Hodapp K. W., Wainscoat R. J. 1994, ApJ 434, 114
- De Propriis R., Eisenhardt P. R., Stanford S. A., Dickinson M. 1998, ApJ 503, L45
- De Propriis R., Stanford S. A., Eisenhardt P. R., Dickinson M., Elston R. 1999, AJ submitted (astro-ph/9905137)
- Dickinson M. 1995, ASP Conf. Ser. 86, 283
- Dickinson M. 1997a, in HST and the High Redshift Universe, ed N. R. Tanvir, A. Aragón-Salamanca, J.V. Wall (World Scientific, Singapore) p207
- Dickinson M. 1997b, in The Early Universe with the VLT, ed J. Bergeron (Springer, Berlin) p274
- Driver S. P., Phillipps S., Davies J. I., Morgan I., Disney M. J. 1994, MNRAS 268, 393
- Driver S. P., Couch W. J., Phillipps S. 1998, MNRAS 301, 369
- Ferguson H. C., Babul A. 1998, MNRAS 296, 585
- Franceschini A., Silva L., Fasano G., Granato L., Bressan A., Arnouts S., Danese L. 1998, ApJ 506, 600
- Hall P. B., Green R. F. 1998, ApJ 507, 558
- Kashikawa N., Shimasaku K., Yagi M., Yasuda N., Doi M., Okamura S., Sekiguchi M. 1995, ApJ 452, L99
- Kauffmann G., Charlot S. 1998, MNRAS 297, L23
- Kauffmann G., White S. D. M., Guiderdoni B. 1993, MNRAS 264, 201
- Kepner J. V., Babul A., Spergel D. N. 1997, ApJ 487, 61
- Kristian J., Sandage A., Katem B. 1974, ApJ 191, 43
- McLeod B. A., Bernstein G. M., Rieke M. J., Tollestrup E. V., Fazio G. G. 1995, ApJS 96, 117
- Metcalfe N., Godwin J. G., Peach J. V. 1994, MNRAS 267, 431
- Minezaki T., Kobayashi Y., Yoshii Y., Peterson B. A. 1998, ApJ 494, 111

- Motohara K., Maihara T., Iwamuro F., Oya S., Imanishi M., Terada H., Goto M., Iwai J., et al. 1998, Proc. SPIE 3354, 659
- Moustakas L. A., Davis M., Graham J. R., Silk J., Peterson B. A., Yoshii Y. 1997, ApJ 475, 445
- Rosati P., Stanford S. A., Eisenhardt P. R., Elston R., Spinrad H., Stern D., Dey A. 1999, AJ 118, 76
- Sandage A., Binggeli B., Tammann G. A. 1985, AJ 90, 1759
- Secker J., Harris W. E. 1996, ApJ 469, 623
- Schechter P. 1976, ApJ 203, 297
- Smail I., Dickinson M. 1995, ApJ 455, L99
- Smith R. M., Driver S. P., Phillipps S. 1997, MNRAS 287, 415
- Spinrad H., Djorgovski S. 1984, ApJ 280, L9
- Stanford S. A., Elston R., Eisenhardt P. R., Spinrad H., Stern D., Dey A. 1997, AJ 114, 2232
- Thompson L. A., Gregory S. A. 1993, AJ 106, 2197
- Totani T., Yoshii Y. 1998, ApJ 501, L177
- Wilson G. , Smail I., Ellis R. S., Couch W. J. 1997, MNRAS 284, 915
- Yamada T., Tanaka I., Aragón-Salamanca A., Kodama T., Ohta K., Arimoto N. 1997, ApJ 487, L125
- Yan L., McCarthy P. J., Storrie-Lombardi L. J., Weymann R. J. 1998, ApJ 503, L19

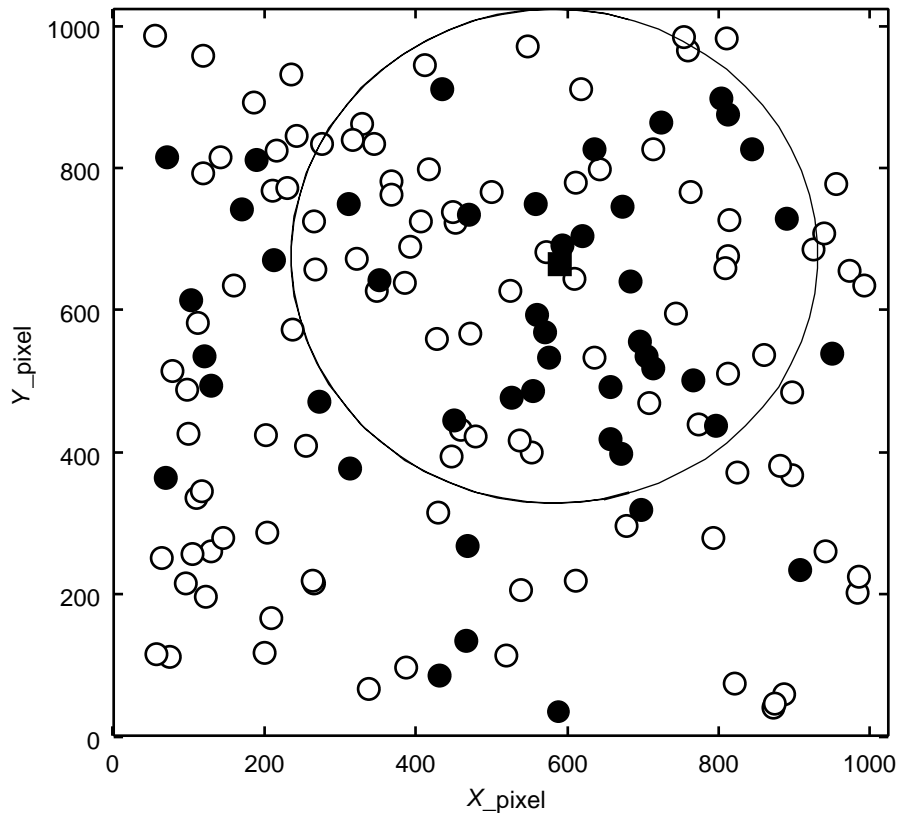


Fig. 1. Distribution of the 146 detected objects on the sky. The position angle of the figure is 218° . 3C 324 is shown by the filled square. The objects with $K < 20$ are shown by the filled circles and those with $K > 20$ by the open circles. The large circle indicates the “cluster” region within $40''$ from 3C 324.

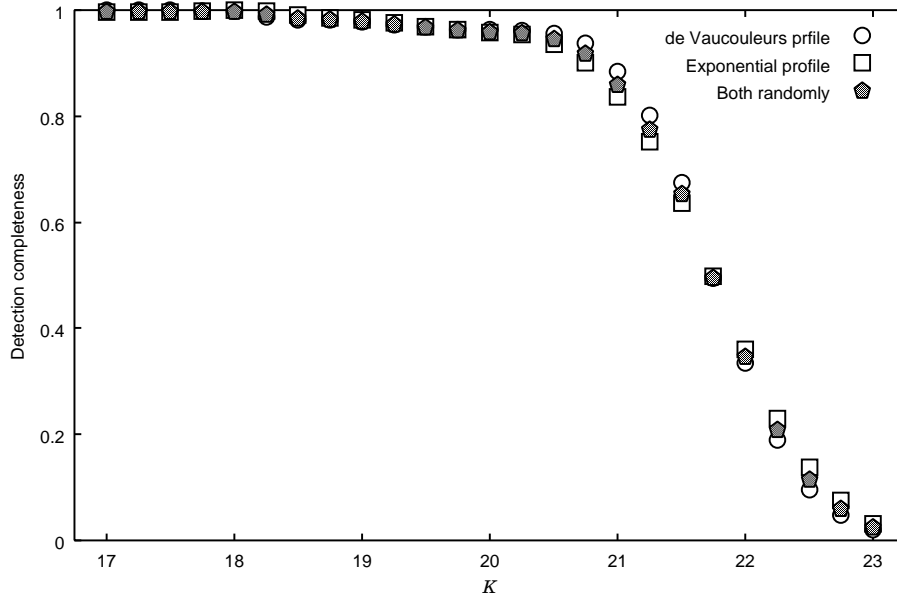


Fig. 2. Detection completeness as a function of the apparent magnitude derived from the simulation (see text). Each symbol represents the adopted profiles of the artificial galaxies; de Vaucouleurs profile (open circle), exponential profile (open square), average of both profiles (shaded pentagon), respectively.

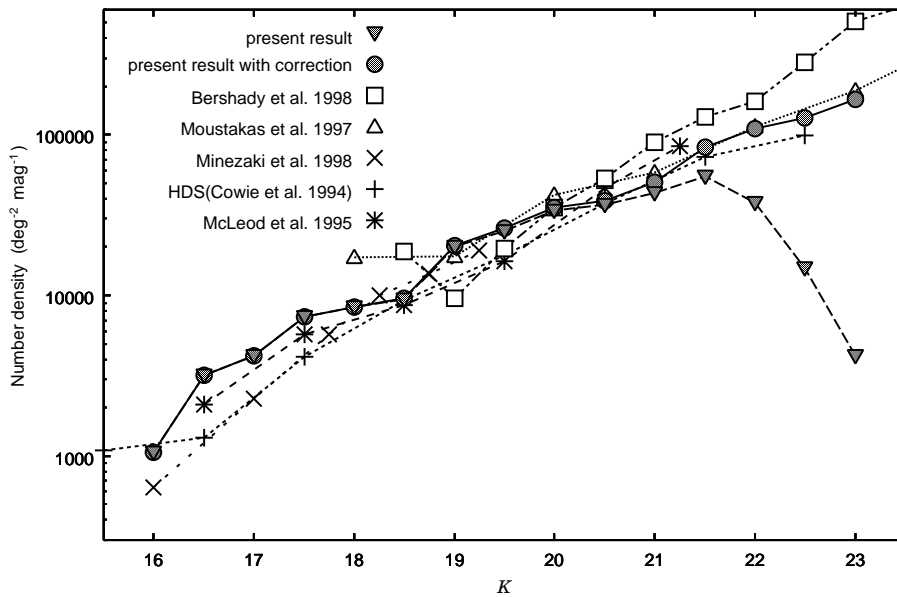


Fig. 3. K -band number counts of the galaxies in the 3C 324 region. The observed counts (shaded triangles) as well as the incompleteness-corrected counts (shaded circles) are shown. The galaxy counts in the general field taken from literatures are also plotted.

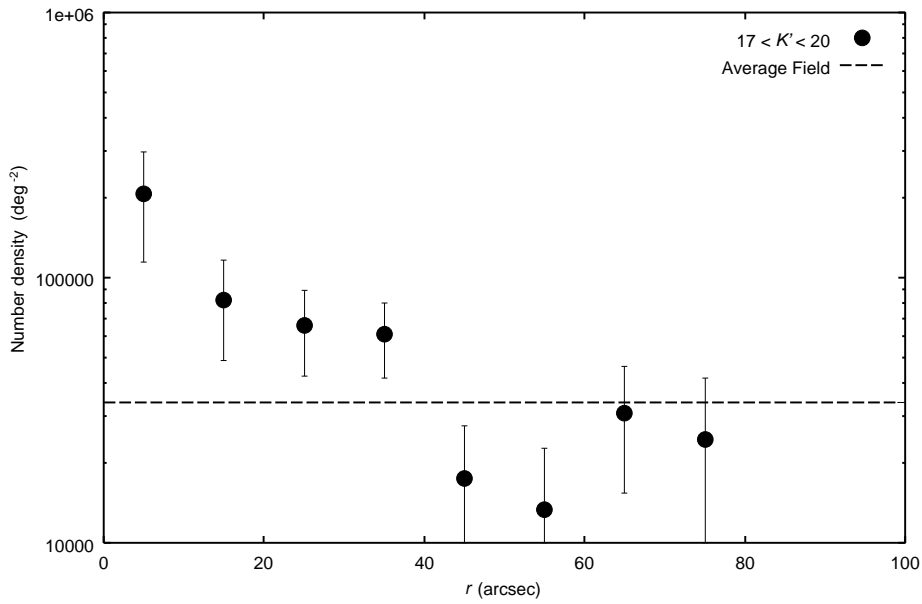


Fig. 4. Surface number density profile of the galaxies with $17 < K < 20$ as a function of the radius from 3C 324. The dashed line represents the averaged surface number densities in the field shown in figure 2. The error-bars represent the square root of the number of detected galaxies.

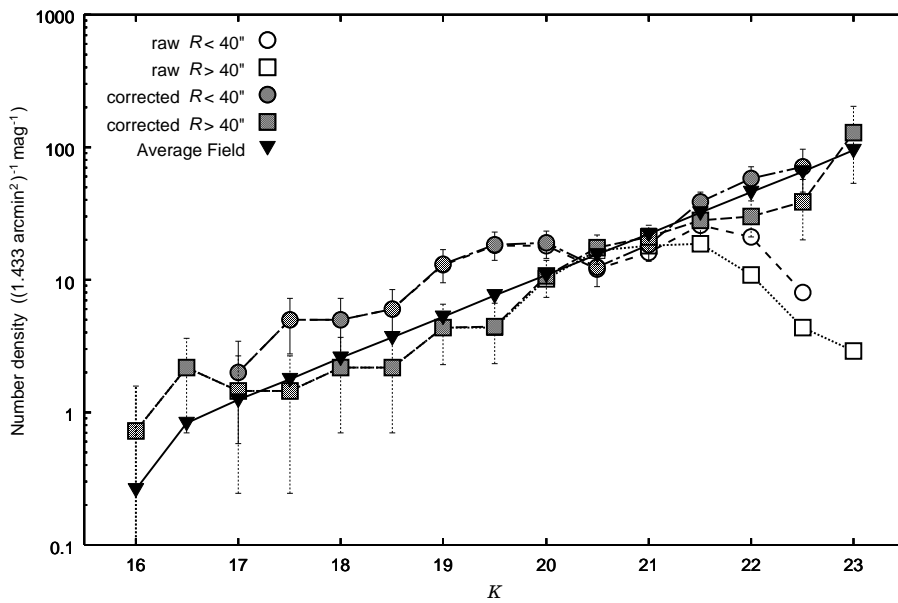


Fig. 5. Corrected (shaded symbol) and raw (open symbol) K -band number counts of the “cluster” and the “outer” regions. The filled triangles show the approximate average field counts. The number density is normalized by the area of the “cluster” region.

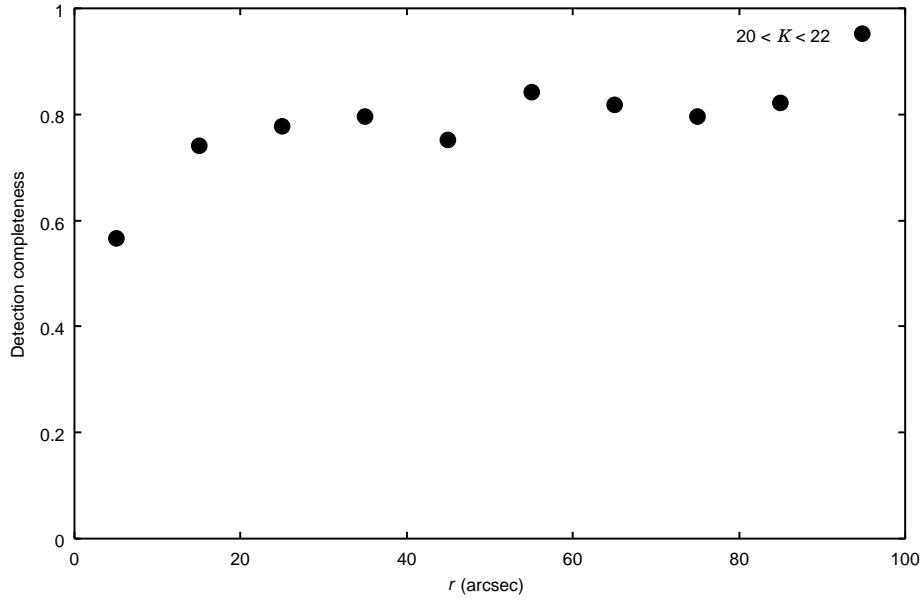


Fig. 6. Detection completeness as a function of the distance from the 3C 324 for the galaxies with $20 < K < 22$.

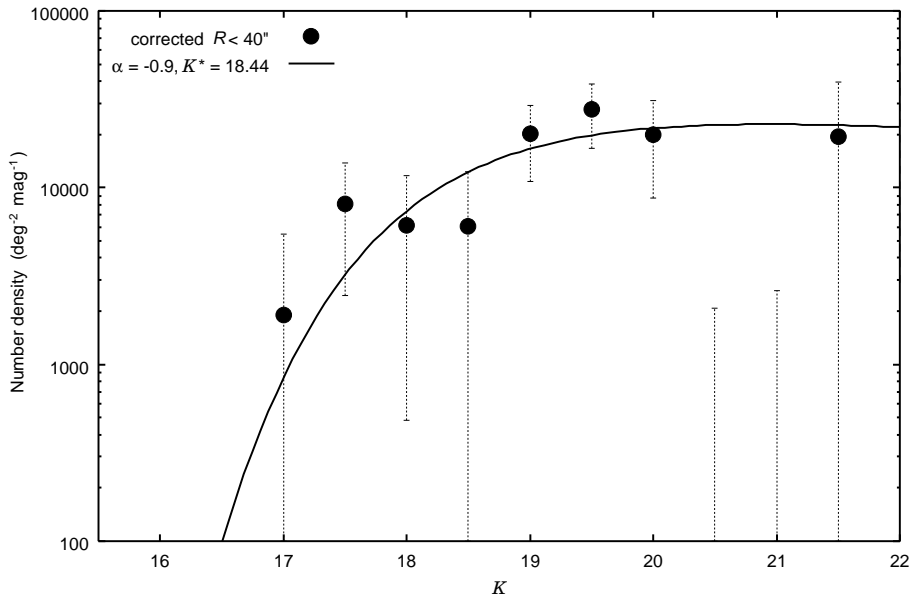


Fig. 7. Luminosity function of the cluster region. The solid line is the Schechter function fitted to the points between $K = 17$ and 20 mag. Note that the observed values at $K = 20.5$ and 21.0 are negative.

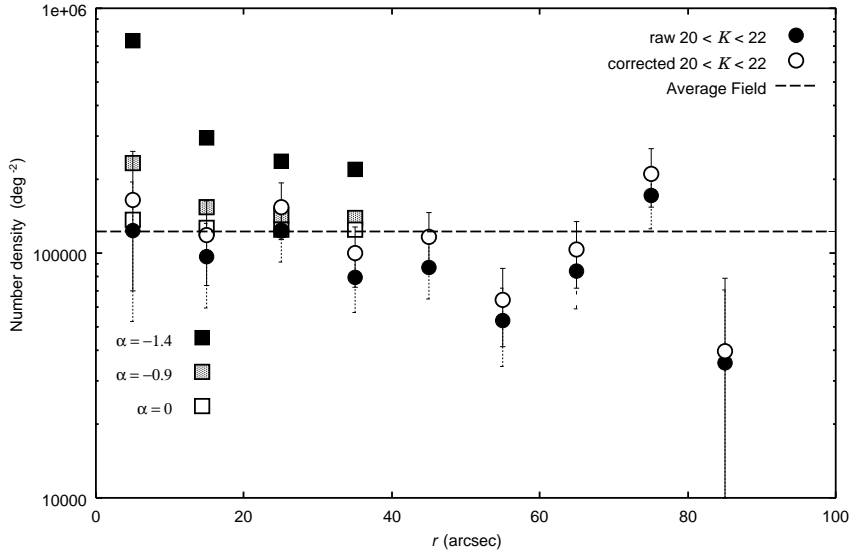


Fig. 8. Raw (filled circles) and the corrected (open circles) surface number density profile of the galaxies with $20 < K < 22$ in function of the radius from 3C 324. The dashed line represents the averaged surface number densities in the field shown in figure 2. For a comparison, we also show the expected profiles derived from the counts at $K = 17-20$ mag assuming the Schechter function and various values of the faint-end slope (squares).

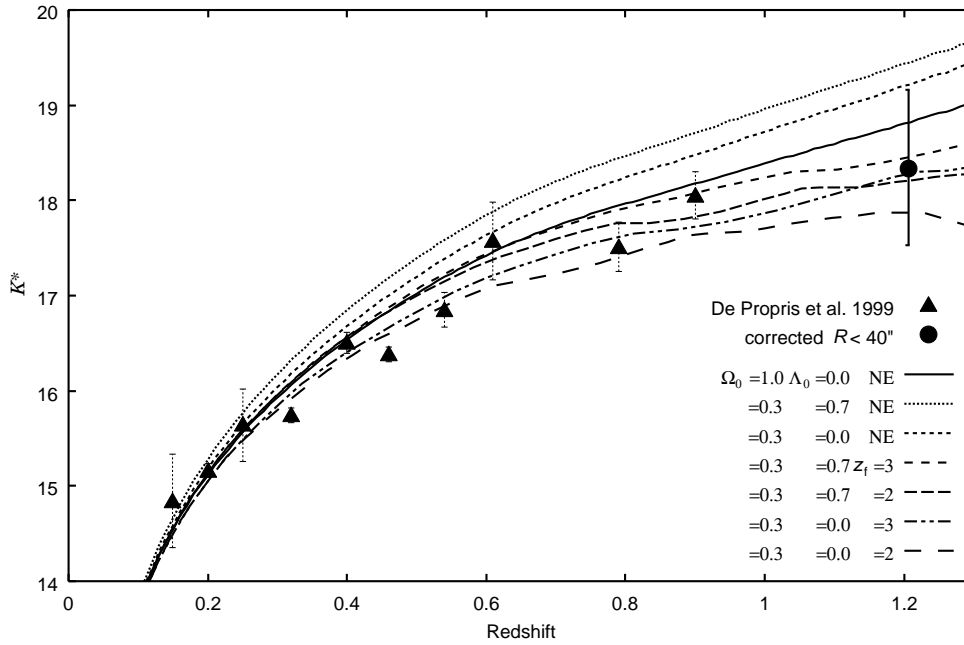


Fig. 9. K^*-z Hubble diagram for the clusters at $z = 0.1-0.9$ studied by De Propriis et al. (1999) and the 3C 324 cluster. Lines represent galaxy models calculated using GISELL96 (see text) under the various set of the cosmological parameters, Ω_0 and Λ_0 . $H_0 = 65 \text{ km s}^{-1} \text{ Mpc}^{-1}$ is adopted.